TECHNISCHE UNIVERSITÄT DRESDEN
Facultad de Ciencias Astronómicas y Geofísicas
UNIVERSIDAD NACIONAL DE LA PLATA
CONICET
Consejo Nacional de Investigaciones Científicas y Técnicas

European Geosciences Union
General Assembly 2016
Vienna | Austria | 17–22 April 2016

Tides and lake-level variations in the great Patagonian lakes: Observations, modelling and geophysical implications

Eric Marderwald[1,2,3], Andreas Richter[1,2,3], Martin Horwath[3], Jose Luis Hormaechea[1], Andreas Groh[3] and Mirko Scheinert[3]

[1]Facultad de Ciencias Astronómicas y Geofísicas, Universidad Nacional de La Plata, Argentina [2]CONICET, Argentina [3]Institut für Planetare Geodäsie, Technische Universität Dresden, Germany

Introduction

- The glacial-isostatic adjustment (GIA) in Patagonia to past ice-mass changes (Ivins & James 2004; Klemann et al. 2007) is of particular interest in the context of the determination of the complex regional rheology related to plate subduction in a triple-junction constellation.
- The elastic responce of the solid earth to ongoing ice-mass loss adds to the crustal uplift observable at the patagonian icefields today (Dietrich et al. 2010; Lange et al. 2014).
- Using lake tide observations in Lago Fagnano (Tierra del Fuego) Richter et al. (2009) revealed deviations from conventional elastic earth models that document an amplification of ocean tidal loading effects. Morover, elastic deformations due to water level changes in the lakes surrounding the icefields and the ocean surrounding Patagonia affect the determination of glacial-isostatic uplift rates from GPS observations.
- In this context we investigate the Patagonian lakes (Fig. 1): Lago Argentino, Lago Viedma, Lago San Martín/O'Higgins and Lago Buenos Aires/General Carrera.

Lake-level observations

- We present pressure tide-gauge records (Fig. 2) from two sites in Lago Argentino (Richter et al. 2016): Punta Bandera (site C, 2.5 years) and Bahía Toro (site W, 1 year). These high-resolution records are complemented by water level data of the Argentine National Hydrometeorological Network (BDHI, 2015): El Calafate (Lago Argentino, site E), Brazo Rico (Lago Argentino, site R), Bahía Túnel (Lago Viedma), Brazo Maipú (Lago San Martín/O'Higgins) and Los Antiguos (Lago Buenos Aires/General Carrera) (Tab. 1 and fig. 3).
- Lake-level changes are dominated by a seasonal cycle exceeding 1 m in amplitude, in addition a daily period is included that reflects the response to melt water influx from surrounding glaciers (Fig. 3).
- Movement of the water body in these lakes is dominated by surface seiches reaching 20 cm in amplitude (Fig. 4).
- Sporadic lake-volume jumps are caused by bursting of the ice dam of Perito Moreno glacier (Fig 5).
- A harmonic tidal analysis of the lake-level time series from Lagos Argentino and Viedma yields amplitude and phase of the lake tides for the four major tidal constituents M2, S2, O1 and K1. The maximum amplitude, corresponding to the semi-diurnal lunar tide M2 in Lago Argentino, amounts to 3 mm (Fig. 7).

Lake-tide modelling

- Theoretical amplitudes and phases of seven tidal constituents (Q1, O1, P1, K1, N2, M2 and S2) for the four lakes are modelled accounting for the contributions of both the body tides and the ocean tidal loading (Marderwald 2014). Both contributions involve a deformation of the surface of the solid earth (i.e., lake bed) and of the equipotencial surfaces of the gravity field (to which the water surface adjusts) (Fig. 6).
- For the load tide computation the global ocean tide model EOT11a (Savcenko and Bosch, 2012) and the Gutenberg-Bullen A earth model (Farrell, 1972) was applied, and the conservation of water volume is taken into account.
- The results show that lake tides generate anti-clockwise gyres about an amphidrome close to the geometric centre of the lake area. Maximum amplitudes are located at the lake's most distant points from this amphidrome. The pattern of amplitudes and phases are similar for all constituents. The predicted maximum amplitudes for the four major tidal constituents and morphometric parameters are given in Tab. 2.

Geophysical implications

- The comparison of the tidal signal extracted from the lake-level observations with model predictions in Lago Argentino and Lago Viedma indicates a phase shift which is most likely explained by an 1 hour phase lag of the employed global ocean tide model at the highly fragmented Pacific coast (Fig 7).
- Therefore, the lake-tide observations do not allow an unambiguos validation of elastic earth models for the Southern Patagonian Icefied region.
- Precise long-term lake-level records may provide a useful observable to validate models of glacial-isostatic adjustment in the region of the Southern Patagonian Icefield (e. g. Lange et al., 2014).
- Our results allow a tentative prediction of characteristics of lake-level variations in the other great Patagonian lakes, but also reveal optimal sites for a future operation of tide gauges dedicated to monitor secular lake-level changes and relative crustal deformation. They allow to quantify and correct the loading effect of lake-level variations while determining glacial-isostatic uplift rates.

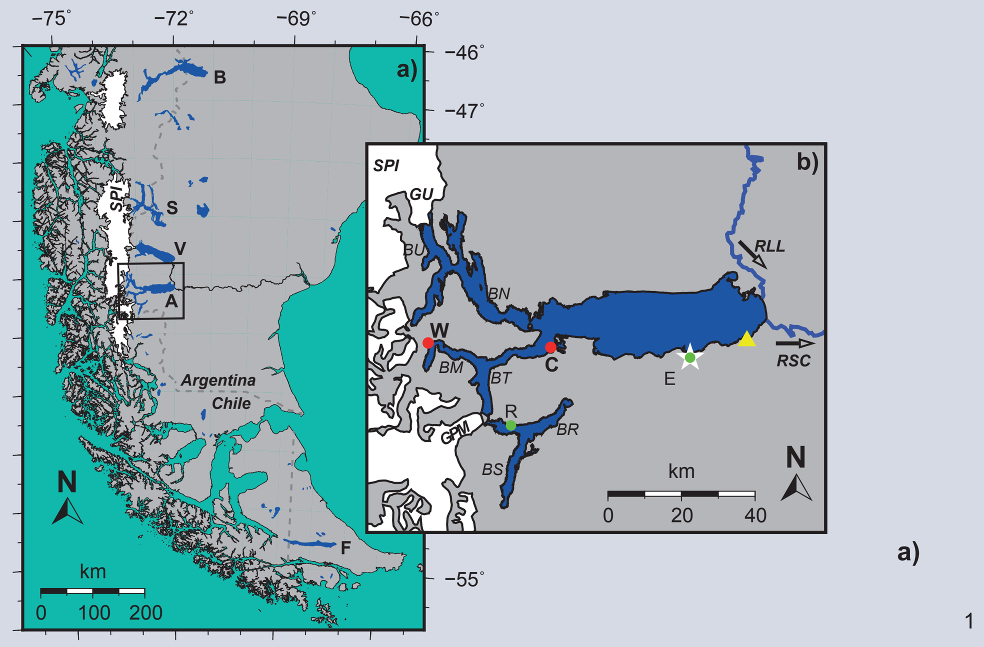

Figure 1: (a) Map of southern Patagonia with the great Patagonian lakes: Lago Buenos Aires/General Carrera (B), Lago San Martín/O'Higgins (S), Lago Viedma (V), Lago Argentino (A) and Lago Fagnano (F). White patches: Northern and Southern Patagonian Icefields (SPI).
(b) Detail map of the Lago Argentino. Red dots: tide gauge deployed at sites C and W during this project; green dots: tide gauge data from BDHI (2015) (R: Brazo Rico, E: El Calafate); yellow triangle: meteorological station of Servicio Meteorológico Nacional at El Calafate airport; white star: city of El Calafate; Rivers: Río La Leona (RLL) and Río Santa Cruz (RSC); white area: Southern Patagonian Icefield (SPI) and glaciers (GU, Upsala glacier; GPM, Perito Moreno glacier); parts of Lago Argentino: BU, Brazo Upsala; BN, Brazo Norte; BM, Brazo Mayo; BT, Brazo de los Tempanos; BR, Brazo Rico; BS, Brazo Sur.

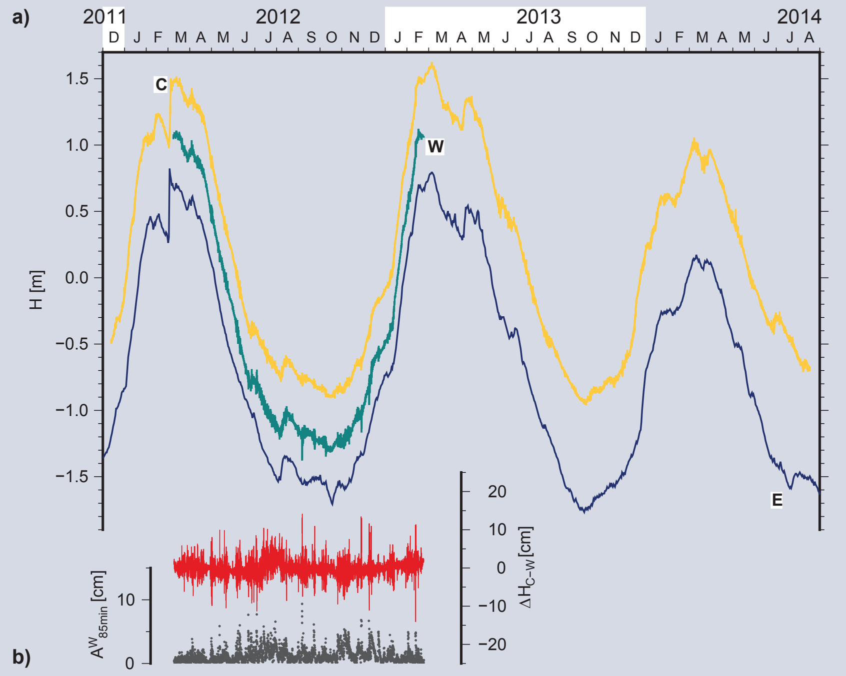

Figure 2: (a) Lake-level time series derived from pressure tide gauge records at sites C (yellow) and W (grey); lake-level data for site E (blue) from BDHI (2015).
(b) For the period of simultaneous tide gauge operation, the time series of differential lake-level changes between sites C minus W are shown in red; dark grey dots: time series of the surface seiches amplitude at site W for the fundamental seiches mode with a period of 85 min.

Table 1: Lake-level records in Lago Argentino (sites C-R) and in other great Patagonian lakes included in the analysis.

Site	Location	Lat. S	Lon. W	Start	End	Rate
C	Punta Bandera	50°18.0′	72°47.8′	12/12/2011	08/03/2012	5 min
				09/03/2012	24/02/2013	10 min
				24/02/2013	17/08/2014	15 min
W	Bahía Toro	50°17.3′	73°15.9′	08/03/2012	22/02/2013	10 min
E*	El Calafate	50°19.2′	72°15.7′	08/01/1992	30/10/2014	24 h
R*	Brazo Rico	50°29.4′	72°57.0′	15/11/1991	30/10/2014	24 h
Lago Viedma*	Bahía Túnel	49°23.7′	72°52.2′	01/03/2010	23/09/2010	24 h
				24/09/2010	15/11/2010	4 h
				15/11/2010	22/09/2011	1h
				23/09/2011	30/09/2014	4 h
Lago Buenos Aires/General Carrera*	Los Antiguos	46°32.3′	71°36.6′	18/09/2008	29/09/2014	8 h
Lago San Martin/O´Higgins*	Brazo Chacabuco	49°07.4′	72°29.1′	01/03/2010	29/09/2014	24 h

*Data sets retrieved from BDHI (2015).

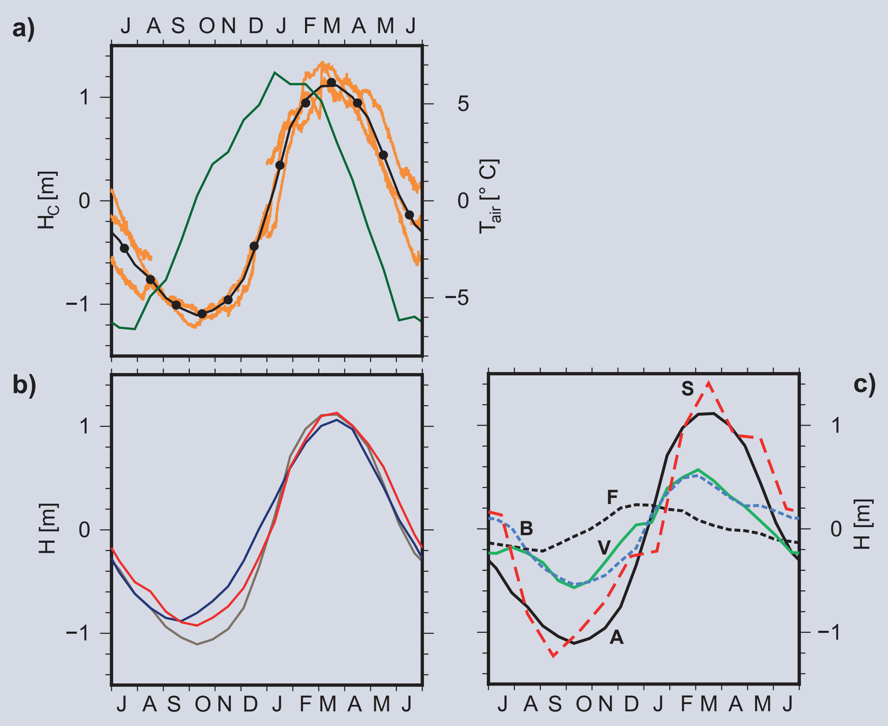

Figure 3: Stacked annual lake-level signal (July 1 June 30).
(a) Original (orange) and stacked mean annual lake-level signal, H_C, observed at site C; green line: stacked mean annual air temperature observed at El Calafate (2010-2014), T_{air}; letters indicate the months.
(b) Comparison of the stacked mean annual lakelevel signal at site C (red) with the corresponding lake-level signal derived for site E for the period 1992-1996 (blue) and 2010-2014 (brown).
(c) Comparison of the stacked mean annual lake-level signal derived at site C for Lago Argentino (A, black) with the corresponding signals for Lagos San Martín/O'Higgins (S, red; BDHI, 2015), Buenos Aires/General Carrera (B, blue; BDHI, 2015), Viedma (V, green; BDHI, 2015) and Fagnano (F, black dashed; Richter et al., 2010).

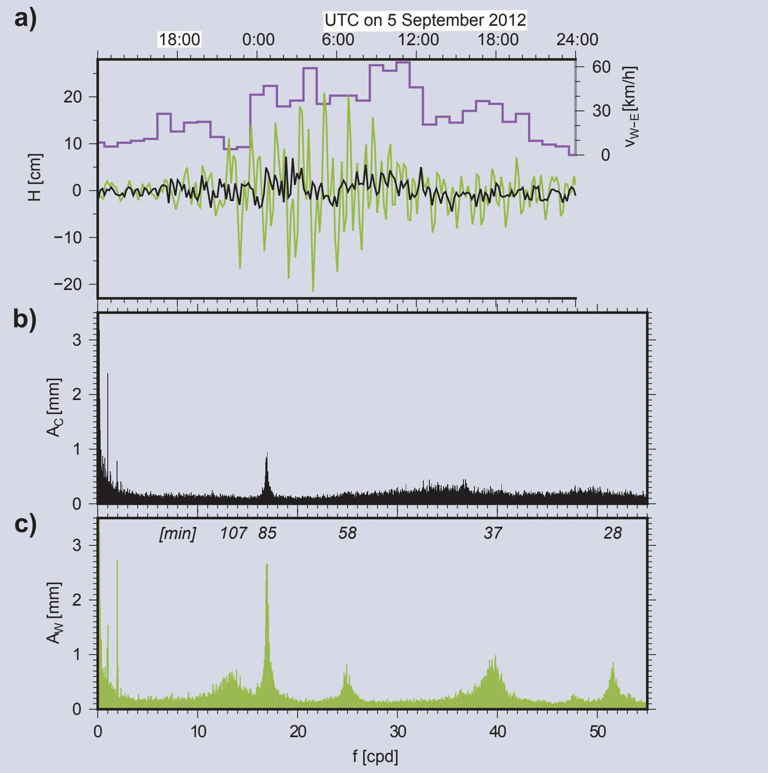

Figure 4: Surface seiches observed in Lago Argentino.
(a) Simultaneous lake-level time series at sites C (black) and W (green) from late 4 to 5 September 2012 showing the onset and evolution of a seiches series; jagged violet line: east-west wind velocity component $v_{W\text{-}E}$ observed at El Calafate.
(b) Amplitude spectrum of the lake-level variations observed at site C throughout the common observation period at sites C and W; the prominent peak at frequency 17 cpd (cycles per day) represents the fundamental surface seiches mode with a period of 85 min; large amplitudes at low frequencies are truncated.
(c) Amplitude spectrum for site W analogous to (b); for the frequencies with significant seiches amplitudes the corresponding period (min) is included.

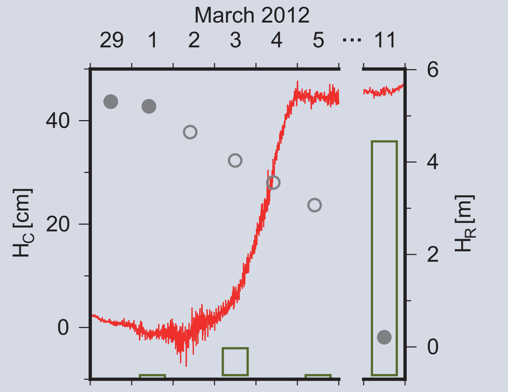

Figure 5: Lake-level time series covering the singular event of the ice dam burst of Perito Moreno glacier.
Lake-level variation observed at site C, H_C (red, left axis annotation) during and after the ice dam burst on March 2, 2012; grey dots: simultaneous lake-level readings at site R in Brazo Rico H_R (axis annotation to the right; BDHI, 2015); open circles: implausible lake-level data likely resulting from linear interpolation; the relative axis scale for H_C and H_R corresponds to the ratio of surface area between the proper Lago Argentino and Brazo Rico/Sur of 1:11; green bars indicate rainfall as observed at El Calafate meteorological station (larger bar on March 11 corresponds to 5 mm).

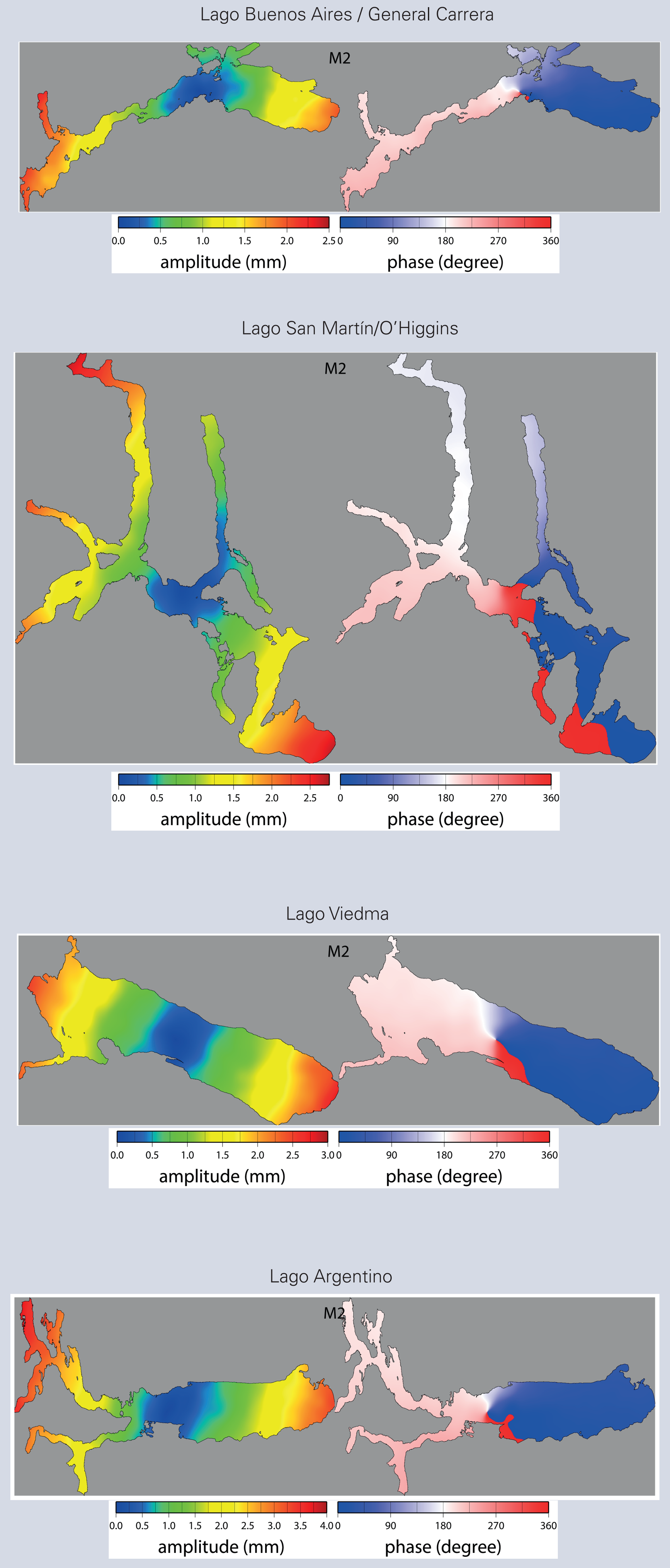

Figure 6: Theoretical amplitude and phase of the tidal constituent M2 for the four lakes.

Table 2: Morphometric parameters for the great Patagonian lakes. Amplitudes of the principal tidal constituents M2, S2, K1, O1 predicted by lake tide models. For the M2 constituent also the phase lags (relative to the 0° meridian) and the contributions of body tide (Body) and load tide (Load) are included.

	Lago Argentino		Bs. Aires/Gral. Carrera		San Martín/O'Higgins		Viedma		Fagnano	
Length (km)	99.8		132.6		103.3		79.1		104.1	
Width max. (km)	33.6		36.6		54.0		35.8		10.0	
Area total (km2)	1329.6		1803.0		1034.1		1021.1		600.9	
Area islands (km2)	3.0		14.8		9.7		0.1		0.0	
Shore length (km)	697		744		838		285		261	
Maximum amplitudes (and phases) according to lake tide models:										
M2 (mm, °)	3.77	195.6	2.27	196.0	2.66	4.7	2.76	19.0	4.97	346.8
Body	1.79	209.8	2.70	253.4	1.59	176.9	1.36	42.0	1.41	50.1
Load	2.20	188.6	1.43	123.2	1.31	352.5	1.59	1.0	4.52	330.7
S2 (mm, °)	1.2		1.13		0.96		0.86		1.73	
K1 (mm, °)	1.41		1.86		1.05		1.10		1.7	
O1 (mm, °)	1.06		1.51		0.82		0.84		1.04	

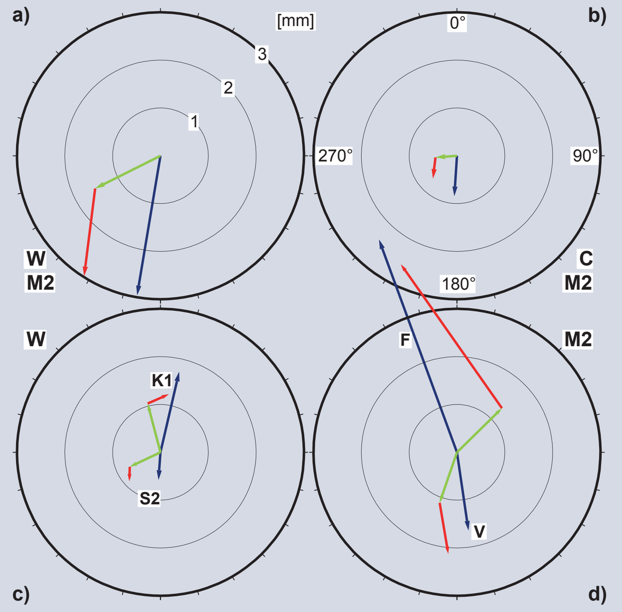

Figure 7: Phasor plots of the observed vs modelled lake tide signals.
(a) M2 lake tide signal extracted from the lake-level observations at site W (blue); light green and red vectors: modelled contributions of body tide and load tide, respectively, to the theoretical lake tide signal at this site. For a perfect agreement between observations and model the vector sequence would be closed.
(b) Same as (a) for site C.
(c) For the K1 and S2 tidal constituents the lake tide signals extracted from the lake-level observations at site W (blue) and the model contributions of body tide and load tide (green and red) are shown.
(d) For Lago Fagnano (F, site C in Richter et al., 2009) and Lago Viedma (V, Bahía Túnel; BDHI, 2015) the observed (blue) M2 lake tide signal and the modelled contributions of body tide and load tide (light green and red) are shown.

References

Dietrich R. et al. (2010). Rapid crustal uplift in Patagonia due to enhanced ice loss. Earth Planet. Sci. Lett. 289:22-29.
Farrell, W. E., (1972). Deformation of the Earth by Surface Loads. Rev. Geophy. Space Phy., 10(3):761- 797.
Ivins, E., James, T., 2004. Bedrock response to Llanquihue Holocene and present-day glaciation in southernmost South America. Geophys. Res. Lett. 31 (L24613). Doi:10.1029/2004GL021500.
Klemann, V., E. R. Ivins, Z. Martinec, and D. Wolf (2007), Models of active glacial isostasy roofing warm subduction: Case of the South Patagonian Ice Field, J. Geophys. Res., 112, B09405, doi: 10.1029/2006JB004818.
Lange, H., Casassa, G., Ivins, E. R., Schröder, L., Fritsche, M., Richter, A., Groh, A., Dietrich, R., (2014). Observed crustal uplift near the Southern Patagonian Icefield constrains improved viscoelastic Earth models. Geophysical Research Letters, DOI: 10.1002/2013GL058419.
Marderwald ER, 2014. Modelado de las mareas de grandes lagos patagónicos. Licenciatura thesis, Universidad Nacional de La Plata, Argentina.
Richter, A., Marderwald, E., Hormaechea, J.L., Mendoza, L., Perdomo, R., Connon, G., Scheinert, M., Horwath, M., Dietrich, R. (2016): Lake-level variations and tides in Lago Argentino, Patagonia: insights from pressure tide gauge records. Journal of Limnology, doi:10.4081/jlimnol.2015.1189.
Richter A, Hormaechea JL, Dietrich R, Perdomo R, Fritsche M, Del Cogliano D, Liebsch G, Mendoza L, 2009. Anomalous ocean load tide signal observed in lake-level variations in Tierra del Fuego. Geophys. Res. Lett. 36:L05305.
Savcenko, R., and W. Bosch (2012), EOT11a - Empirical Ocean Tide Model from Multi-Mission Satellite Altimetry. Deutsches Geodätisches Forschungsinstitut (DGFI), Munich, Report Number 89.

Contact:
emarderwald@fcaglp.unlp.edu.ar

This work is supported by DAAD/ALEARG promotion 2015 (57186730), CONICET and German Research Foundation (DFG) project RI - 2340/1 - 1.